

# Thermodynamic Modeling of Binary Binders with Agricultural Residues for Hydration Analysis



This work is licensed under a Creative Commons Attribution 4.0 International License

N. S. Ajeeshkumar\* and K. L. Radhika

Department of Civil Engineering,  
University College of Engineering,  
Osmania University, Hyderabad,  
Telangana, India

doi: <https://doi.org/10.15255/CABEQ.2024.2339>

Original scientific paper  
Received: May 30, 2024  
Accepted: March 4, 2025

Supplementary cementitious materials (SCMs), such as fly ash, blast furnace slag, rice husk ash (RHA), and sugarcane bagasse ash (SBA), are increasingly used to promote sustainable construction practices. However, understanding how the chemical composition, fineness, reactive phases, and pore solution content of SCMs affect the reaction process and hydration of cement is challenging. Researchers are developing models, including thermodynamic modelling (TDM), to better understand these effects. TDM is a useful tool for predicting the composition of pore solution and understanding the composition of hydrated cement and SCMs. This study investigates two types of ordinary Portland cement (OPC I and OPC II) with varying chemical and mineral compositions mixed with two SCMs (RHA and SBA). Using TDM, the impact of cement content on hydrate generation in binary mixes is studied. The results revealed that OPC I and OPC II hydration models predicted CSH gel, ettringite, hydrotalcite, calcite, and portlandite. In comparison to OPC I, OPC II predicts 21 % more CSH gel and 25 % less hydrogarnet. The study also found that jennite-like CSH transforms into tobermorite-like CSH with an increase in RHA, and a decrease in portlandite was observed in SBA blended systems. The TDM results were validated using experimental data, providing valuable insights into the type and composition of hydrates that develop during cement hydration and its blends with SCMs.

## Keywords

cement, hydration, modelling, sustainable concrete-making materials

## Introduction

Supplementary cementitious materials (SCMs) are utilized to advance sustainable construction practices, aiming to reduce CO<sub>2</sub> emissions and energy consumption in cement production<sup>1</sup>. These materials encompass various by-products such as fly ash, rice husk ash (RHA), sugarcane bagasse ash (SBA) and more. They have been found to enhance resistance to sulfate-induced deterioration and chloride penetration during extended curing periods, all the while preserving mechanical qualities comparable to cement<sup>2</sup>. Nevertheless, the mineral and chemical composition of the cement greatly influences the development of solid hydration stages and fluid-filled pore networks. Research on hydration processes involving agents such as SCMs, at varying phases, has highlighted their influence on basic components, particle morphology, reaction kinetics, solidification, and mechanical attributes<sup>3</sup>.

To comprehend the impact of diverse elements on hydration, researchers are developing thermody-

namic and geochemical models. Geochemical specification software, like thermodynamic modelling (TDM), is employed to replicate the interplay between solid and liquid constituents throughout the hydration of cement blends, providing a valuable understanding of chemical effects<sup>4</sup>. TDM, coupled with empirical research, has been utilized to explore the impact of the type of SCM and quantity, alterations in water phases, and the structure of hydrates over prolonged reaction periods<sup>5,6</sup>. Additionally, thermodynamic models can forecast the repercussions of cement's mineral and chemical makeup on the interaction between hydration and SCMs over extended durations, with their precision evaluated utilizing practical findings from the hydration process assessments extending for a period of 90 days<sup>7,8</sup>. The aim of this study was to analyze the influence of Portland cement composition on the hydration process in binary blends, particularly when combined with rice husk ash or sugarcane bagasse ash. By using thermodynamic modeling, this research sought to complement experimental findings and provide insights into the optimal blend compositions for enhanced hydration and mechanical performance.

\*Corresponding author: [ajeeshk.phd@uceou.edu](mailto:ajeeshk.phd@uceou.edu)

## Modeling method

In ordinary Portland cement (OPC), soluble alkali sulfates easily dissolve in water, releasing potassium (K), sodium (Na), and sulfur (S) into the water. Minerals with lower solubility undergo partial dissolution until they attain equilibrium with pore fluids<sup>5</sup>. Silicon (Si) and calcium (Ca) combine to form the calcium silicate hydrate (CSH) state, while aluminum (Al), alongside iron (Fe), interacts with hydroxide ions, sulfur (S), carbon (C), and calcium (Ca), leading to the formation of ettringite (AFt) and AFm phase structures along with alternative hydroxide variants. The rate of clinker elements' dissolution determines the amount of Ca, Si, Al, and hydroxide liberated into the liquid medium<sup>9,10</sup>.

Cement hydration occurs via dissolution and precipitation processes, with diverse models explaining how phases in Portland cement undergo hydration at varying rates. For example, the Parrot and Killoh<sup>11</sup> model utilizes equations to define the speed of hydration for different clinker phases, identifying the phase with the slowest rate at the time ( $t$ ) as the dominant factor. The subsequent crucial equations further elucidate these concepts:

Nucleation and growth

$$R_t = \frac{K_1}{N_1} (1 - \alpha_t) (-\ln(1 - \alpha_t))^{(1-N_1)} \quad (1)$$

Diffusion

$$R_t = \frac{K_2 \cdot (1 - \alpha_t)^{2/3}}{1 - (1 - \alpha_t)^{1/3}} \quad \text{or} \quad (2)$$

Formation of the hydration shell

$$R_t = K_3 \cdot (1 - \alpha_t)^{N_3} \quad (3)$$

The formula representing the extent of hydration at a given time, denoted as  $\alpha_t = \alpha_{t-1} + \Delta t \cdot R_{t-1}$ , involves coefficients  $K_1$ ,  $K_2$ ,  $K_3$ ,  $N_1$ , and  $N_3$  from the model proposed by Parrot and Killoh for ordinary portland cement (OPC). This paper utilizes the three empirical expressions (Equations 1 to 3) presented by Parrot and Killoh. Additionally, the influence of the water-to-cement ratio is accounted for using the

function-  $f(w/c) = \left(1 + 04.45 \cdot \left(\frac{w}{c}\right) - 03.330 \cdot \alpha_t\right)^4$ :

for  $\alpha_t > 1.33 (w/c)^{10,11}$ . Insights provided by Parrot and Killoh were considered, along with the integration of surface area effects on initial hydration into our analysis.

In this study, the GEMS-CEM platform was used to thermodynamically model cement systems, allowing for precise calculations of crystalline, aqueous, and gaseous constituents during the pro-

cesses, alongside the assessment of ion reactivity in equilibrium pore solutions.

GEMS V-3.5<sup>12</sup> and CEMDATA V-18<sup>13</sup> were utilized to forecast outcomes in cementitious and pozzolanic processes. Input data for thermodynamic modeling included information on the components and responsiveness of cement and pozzolans, water-cement ratio, and curing. Simulations of hydrated pastes adhered to specific conditions: 21 °C temperature, 100 % relative humidity, and a water-to-cement ratio of 0.5, in line with the experimental conditions. Cement reactions were modeled using Parrot's empirical approach, while the reactivity of RHA and SBA was assessed through fundamental pozzolanic tests<sup>14</sup>. The CSH Q model, known for its representation of a broad range of Ca/Si proportions, was utilized in this study. While thermodynamic modeling proves valuable for predicting cementitious system behavior, it is not without presumptions and constraints. The model assumes system homogeneity, which may not align with real-world scenarios. Furthermore, the assumption of thermodynamic equilibrium might not hold for certain solids, like amorphous CSH and AFm phases, which are metastable. Upon exposure to an open atmosphere, hydrated cement reacts with atmospheric CO<sub>2</sub>, leading to degradation into calcite and related compounds.

Within the field of cement science, rapid mineral formation and dissolution generally allow for the assumption of thermodynamic equilibrium. Nonetheless, slower operations such as clinker dissolution and precipitation of hydrogarnet may not achieve equilibrium promptly, necessitating additional considerations for precise predictions of behavior within cementitious systems.

The accuracy of thermodynamic modeling outcomes relies on the reliability and comprehensiveness of the database. While the revised Cemdata18 dataset is reliable in calculating the properties, composition, quantity, and cement hydrate capacity, there are deficiencies in data concerning alkali, alumina, and water absorption in CSH, which necessitate further information. Additionally, minerals such as quartz, dolomite, goethite, and hematite along with gibbsite, which are absent under standard conditions and within the considered period, should be excluded from the model. Furthermore, the presence of phases such as thaumasite, which are only found in low-temperature conditions, can notably influence cementitious system behavior.

The thermodynamic model predictions were compared against various empirical data findings from X-ray diffraction (XRD), differential thermal analysis (DTA), and thermogravimetric analysis (TGA) of cement mixes, as well as the mechanical strength assessments of mortars. Two different ordi-

nary Portland cement with distinct chemical and mineral compositions were examined using thermodynamics, considering RHA and SBA as SCMs.

Table 1 – Composition of major phases

Composition of major phases in the raw materials (in weight percentages)				
Percentages	OPC-I	OPC-II	RHA	SBA
CaO	62.74	64.28	1.1	4.6
SiO <sub>2</sub>	18.5	19.5	90.8	78.8
Al <sub>2</sub> O <sub>3</sub>	5	5.8	1.8	5.1
Fe <sub>2</sub> O <sub>3</sub>	5	2.6	0.1	1.6
MgO	2.2	1.2	0.2	–
SO <sub>3</sub>	2.4	2.4	–	1.5
Na <sub>2</sub> O	0.4	0.6	–	–
K <sub>2</sub> O	0.2	0.8	2.2	6.8
Loss on ignition	3.1	2.2	3.2	0.4
3CaO·SiO <sub>2</sub>	50	53	–	–
2CaO·SiO <sub>2</sub>	11	14	–	–
3CaO·Al <sub>2</sub> O <sub>3</sub>	4	10	–	–
4CaO·Al <sub>2</sub> O <sub>3</sub> ·Fe <sub>2</sub> O <sub>3</sub>	15	8	–	–
CaCO <sub>3</sub> (Calcite)	4	3	< 1	< 1

The hydration behavior of binary cementitious binders consisting of OPC and either RHA or SBA was investigated. Two types of OPC (OPC-I: SRPC-43 grade, IS 12330; OPC-II: Standard OPC 43, IS 269) were used to study how cement composition affects hydration. The OPC characterized by a low range of C<sub>3</sub>A and alkali (0.4 % Na<sub>2</sub>O and 4 % C<sub>3</sub>A) was labeled as ‘OPC-I’, while the OPC with higher levels (0.6 % Na<sub>2</sub>O and 10 % C<sub>3</sub>A) was designated as ‘OPC-II’. There was also a notable difference in the C<sub>4</sub>AF content between OPC-I (15 %) and OPC-II (8 %). The CaCO<sub>3</sub> levels in SBA and RHA were less than 1 %. The chemical composition of these materials was determined using X-ray fluorescence (XRF), while XRD was used to identify mineral phases. The Bogue formula<sup>15</sup> was applied to calculate clinker phase composition, with adjustments for calcium carbonate content, and these are presented in Table 1. Since Bogue calculations have known limitations, additional experimental techniques were used to verify phase composition and hydration behavior<sup>16,17</sup>. XRD and TGA were conducted on cement samples to identify crystalline phases and quantify portlandite content, bound water, and carbonation effects<sup>18</sup>. The physical properties of the materials, including particle size distribution and specific surface area, were also measured. To reduce the influence of particle morphology on the

relationship between cement and supplementary materials, the particle size distribution of both OPC types was intentionally made comparable. Additionally, reference mixtures comprising solely OPC-I or OPC-II were utilized, along with binary blends consisting of OPC-I combined with 20 % RHA/SBA.

Cement pastes were prepared by mixing OPC with RHA and SBA at a fixed water-to-binder (w/b) ratio of 0.5 to ensure consistency across all samples. The pastes were cast into molds and cured under controlled conditions at 21 °C with 100 % relative humidity to simulate real cement hydration conditions. Hydration was studied at different time intervals, including 1, 2, 7, 28, and 90 days<sup>19</sup>. To accurately analyze hydration reactions, a hydration stopping method was employed using isopropanol drying<sup>20</sup>. This process involved filtering and soaking the samples in isopropanol for 15 minutes to remove free water, followed by drying at 40 °C for 8 minutes. The dried samples were then stored under a nitrogen atmosphere to prevent further reactions before analysis. This method ensured that hydration products remained unaltered during testing<sup>21</sup>. The study also included a specific pozzolanic reactivity test to determine the degree of reaction of RHA and SBA over time. This test provided new data on the reactivity of SCMs under cementitious conditions and helped establish their role in hydration reactions.

The pozzolanic reactivity test was designed to simulate the alkaline environment of hydrated cement using a system containing calcium hydroxide (Ca(OH)<sub>2</sub>), calcium carbonate (CaCO<sub>3</sub>), and potassium hydroxide (KOH). Each sample contained 1 gram of RHA or SBA, 0.25 gram of CaCO<sub>3</sub>, 1 gram of Ca(OH)<sub>2</sub>, and 10 mL of a 0.1 M KOH solution. This system mimicked cement pore solution conditions. Calcium hydroxide served as a source of calcium ions, while CaCO<sub>3</sub> stabilized hydration phases such as monocarbonate. The test was performed at 21 °C, and the hydration reaction was stopped at different intervals using isopropanol drying<sup>21</sup>.

Samples were tested at 1, 2, 7, 28, and 90 days to measure the extent of reaction of RHA and SBA. After hydration was stopped, various analytical techniques were used to determine the degree of reaction of these SCMs. TGA was conducted to measure bound water content and portlandite consumption, which indicated how much RHA or SBA had reacted. XRD analysis identified the crystalline hydration products formed over time. Mass loss calculations were used to estimate the percentage of RHA and SBA that had reacted at each time interval. The results showed that RHA reacted significantly faster than SBA. At 1 day, RHA had reacted 3 %, while SBA had reacted only 2 %. By 2 days, RHA showed a 7 % reaction, while SBA remained

at 2 %. At 7 days, RHA reached 18 % reaction, whereas SBA had reacted only 8 %. By 28 days, RHA reaction had increased to 28 %, but SBA remained low at 9 %. At 90 days, RHA had reacted 65 %, while SBA had reached only 31 %.

Hydration product formation was further analyzed using XRD and TGA, revealing differences in phase evolution between cement blends<sup>22,23</sup>. Compressive strength tests were conducted on mortar samples at 1, 7, 28, and 90 days to evaluate the mechanical performance of different cement blends. To validate the thermodynamic model used in this study, the experimental data obtained from XRD, TGA, and pozzolanic reactivity tests were compared with model predictions. All experimental data obtained in this study were compared with available literature to validate findings and assess the impact of binder composition on hydration, microstructure, and mechanical properties<sup>24</sup>.

## Results and discussion

### Modeling the hydration process of OPC

The simulation of chemical interactions between water and two kinds of Portland cement aimed to investigate the influence of varying combinations on the nature and volume of generated hydrates over the hydration duration, as illustrated in Fig. 1. In both scenarios, essential hydration stages—CSH gel, ettringite, portlandite, and monocarbonate (specifically for OPC-II)—form within the initial hours of curing. Throughout this period, anhydrous components of the OPCs steadily dissolve and the precipitation of siliceous hydrogarnet is predicted. The hydrotalcite phase is also expected in both OPCs but in significantly smaller amounts, estimated at a maximum of 2 grams per 100 grams of cementitious material. Calcite presence was empirically confirmed by XRD at different hydration durations, as shown in Fig. 2, where XRD data for two types of OPCs at 48 hours and three months after curing were calculated. Calcite was calculated to be found in both cement varieties.

Analyzing the modeling results depicted in Fig. 1, TGA analysis detected CSH gel, and XRD analysis conducted at both two and ninety days into the hydration process clearly revealed portlandite, ettringite, and  $C_3(AF)S_{0.84}H$  (siliceous hydrogarnet). The significant qualitative distinction lies in the creation of monocarbonate within OPC-II as a result of increased aluminum and reduced iron levels compared to OPC-I, facilitating its reaction with carbonates. Although the modeling predicted monocarbonate development on the first day of curing for OPC-II, empirical confirmation appeared later, possibly due to sluggish kinetics<sup>5</sup>.

At 90 days of hydration, XRD suggested a slight presence of monosulfate in OPC-I, possibly alongside ettringite. DTA data indicated a slight weight reduction at 180–195 °C, attributed to monosulfate dehydration<sup>25</sup>. However, the calculations did not indicate monosulfate creation due to its thermodynamic instability in the presence of calcite. Fig. 3 illustrates that OPC-II simulations forecasted higher growth of CSH crystal (21 %) and lower formation of siliceous hydrogarnet (25 %) compared to OPC-I. The primary chemical constituents of an OPC led to distinct variations in hydrates. Despite a remarkably similar content of other phases between the two types of cement (as indicated in Table 2), the modeling's estimated volume of CH and CSH gel was compared to values obtained from thermogravimetric analysis and compressive strength.

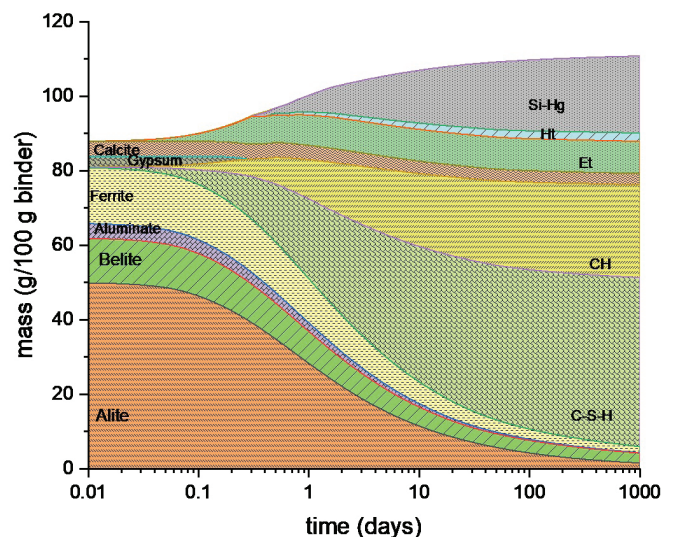


Fig. 1a – OPC-I Hydration model

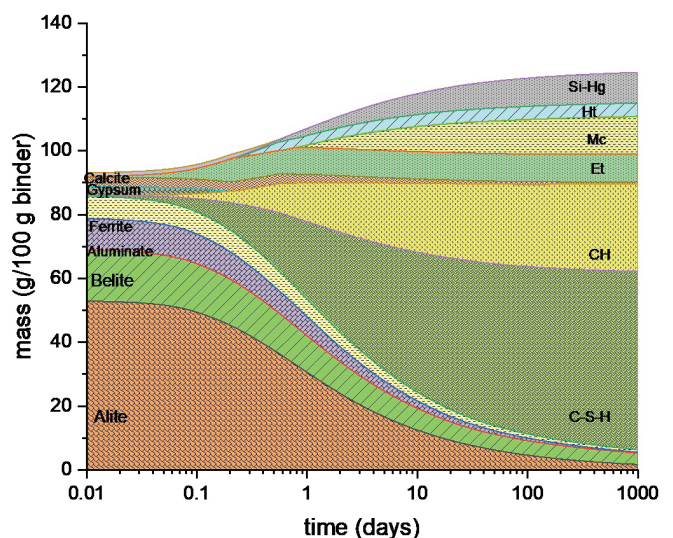


Fig. 1b – OPC-II Hydration model

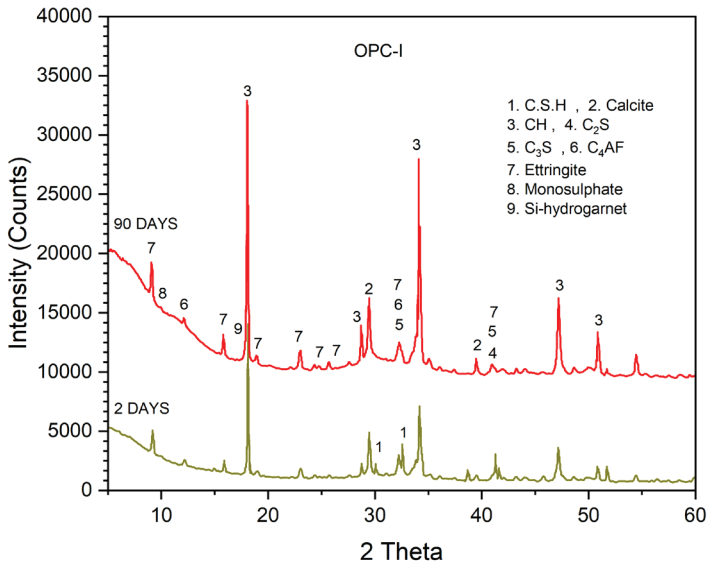


Fig. 2 a – XRD pattern of OPC-I

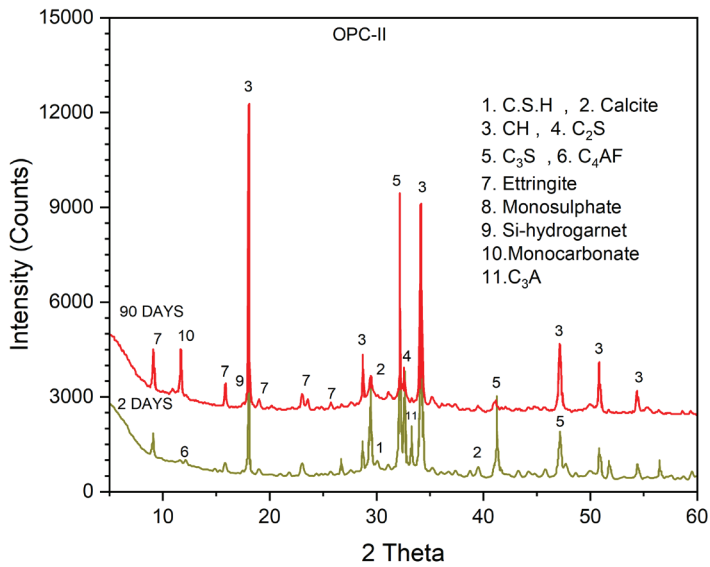


Fig. 2 b – XRD pattern of OPC-II

The modelling slightly overestimated portlandite concentration for both OPC types, with OPC-I consistently having a larger portlandite content than experimental data. Despite simulations predicting a reduced volume of CSH gel and experimental assessments indicating a lower amount of bound water, OPC-I exhibited higher compressive strengths at both 28- and 90-day hydration durations. This implies that components other than spatial arrangement, such as refining the porous structure, might play a role in the noted distinctions.

### Modeling the hydration process of binary blends with SBA/RHA

The objective of this study was to analyze the alterations in the composition of the solid phase re-

Table 2 – TDM forecasted CSH and portlandite, TGA bound water and portlandite (%), compressive strength (MPa)

Title	Time in days	Model (% by mass)		TG/DT (% by mass)		Compressive strength (MPa)
		CSH	CH	Bound Water	CH	
OPC-I	1	18.6	12.4	–	–	14.2
	7	28.2	18.2	15.5	16.1	35.4
	28	32.5	21.3	18.6	17.6	51.6
	90	33.9	22.1	22.1	19.7	56.4
OPC-II	1	18.9	10.9	–	–	21.2
	7	32.8	18	22.1	15.8	37.2
	28	37.1	20.3	23.2	17.2	43.3
	90	37.5	20.1	21.9	17.5	45.9
SBA-I	1	13.2	7.7	–	–	7.8
	7	30.1	9.5	15.2	14.6	31.6
	28	39.6	9.6	15.9	14.4	42.4
	90	40.5	10	17.1	14.4	55.6
RHA-I	1	14.4	6.5	–	–	12.5
	7	30.1	8	14.7	11.3	32.3
	28	45.2	7.4	14.9	11.1	54.9
	90	47.3	7.6	17.1	11.3	60.7

sulting from varying cement contents in blends with RHA and SBA. The investigation commenced with the assessment of the impact of RHA (Fig. 4a). Thermodynamic modeling of blends involving OPC1 and RHA anticipated the formation of primary hydration phases with minimal numerical discrepancies. TDM calculations identified phases with high Ca/Si ratio as ‘jennite-like’ CSH and phases with low Ca/Si ratio as ‘tobermorite-like’ CSH<sup>5</sup>. Adding RHA reduced portlandite levels and increased CSH gel production. As the RHA content increased, the extra SiO<sub>2</sub> present in RHA interacted with ‘jennite-like’ CSH, gradually shifting it towards ‘tobermorite-like’ CSH.

Fig. 3 illustrates that simulations of the RHA1 blend predicted a higher growth of CSH crystals (48 %) and a lower presence of CH (70 %) in comparison to simulations with OPC1. Likewise, RHA1 blend simulations showed increased formation of CSH crystals (27 %) and reduced CH (28 %) in comparison to SBA1 simulations, attributed to the elevated pozzolanic activity of RHA. In terms of quantity, particularly at prolonged hydration durations, the reaction of RHA led to an augmentation

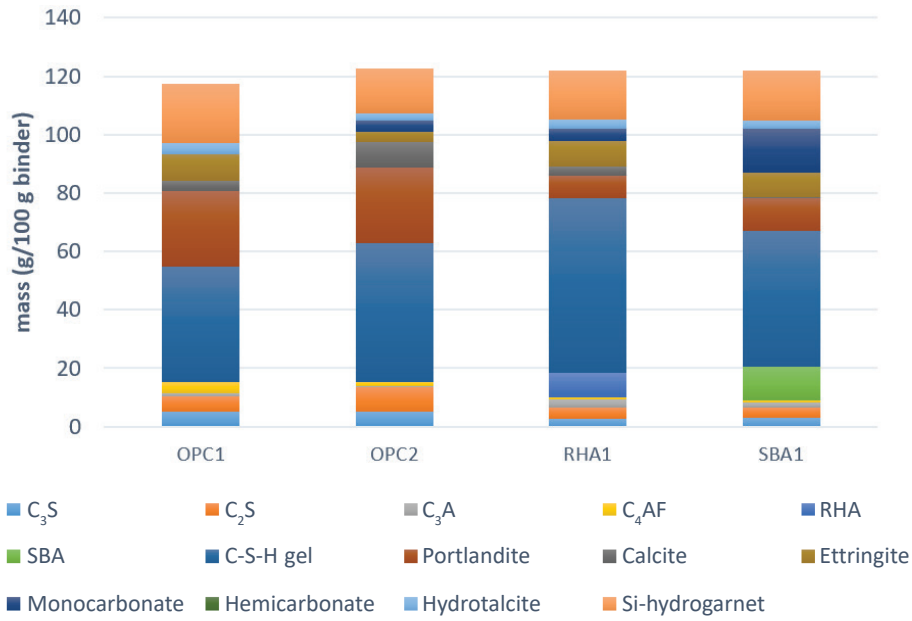


Fig. 3 – Solid phase mass at ninety days

in CSH gel and a reduction in CH content compared to Portland cement, leading to the dual mixture displaying higher compressive strength compared to Portland cement (see Table 2).

The investigation also delved into SBA's impact on hydration (Fig. 4b). Combining cement and SBA resulted in a decrease in portlandite content within the hydrated mixture, exhibiting a less pronounced reduction compared to RHA (Fig. 4a) due to SBA's lower reactivity. SBA, containing 5 % alumina, led to the creation of small amounts of aluminum-rich compounds upon addition to PC. The results highlighted the destabilization of portlandite in the existence of moderate levels of SBA, resulting in increased CSH with a lower Ca/Si ratio. Addi-

tionally, the mixture exhibited the formation of monocarbonates owing to the inclusion of aluminum from SBA, setting it apart from OPC1.

The RHA mixture displayed an elevated level of CSH gel, coupled with a reduced amount of free water. This is credited to the extra CSH gel generated from the interaction with RHA, which possessed a reduced amount of free water compared to the CSH gel produced solely in Portland cement. The diminutive particle size of RHA facilitated their infiltration into the CSH gel pores framework, leading to a more compact gel formation characterized by diminished porosity and enhanced strength. Despite the heightened compressive strength in RHA-mixed compositions, the rise in overall hy-

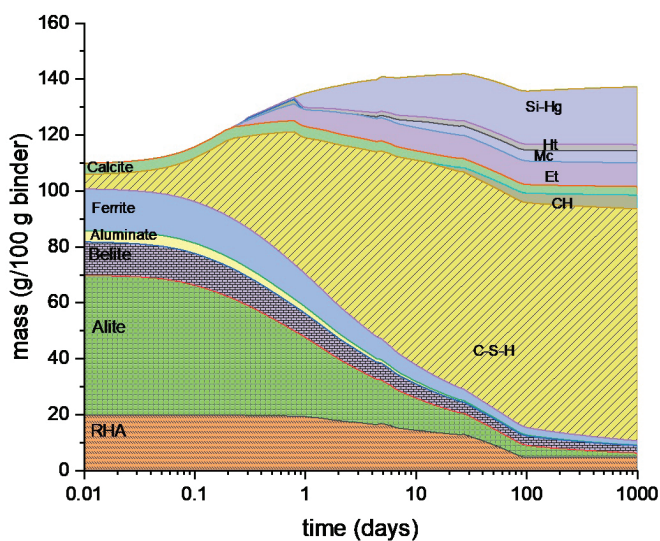


Fig. 4a – OPC – RHA hydration model

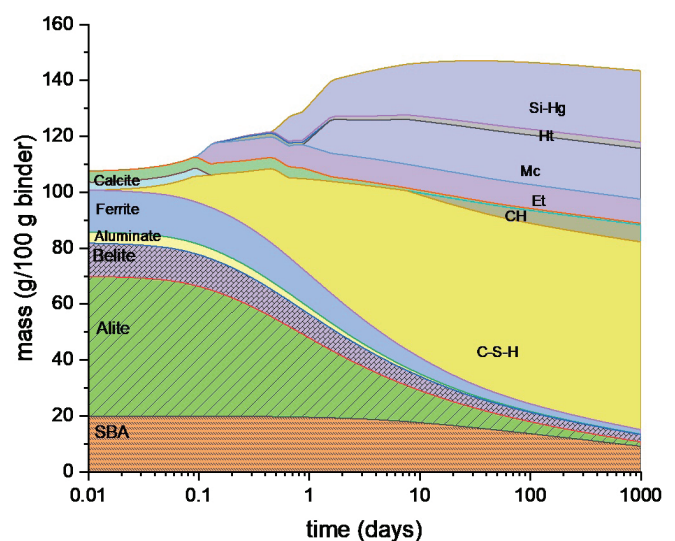


Fig. 4b – OPC – SBA hydration model

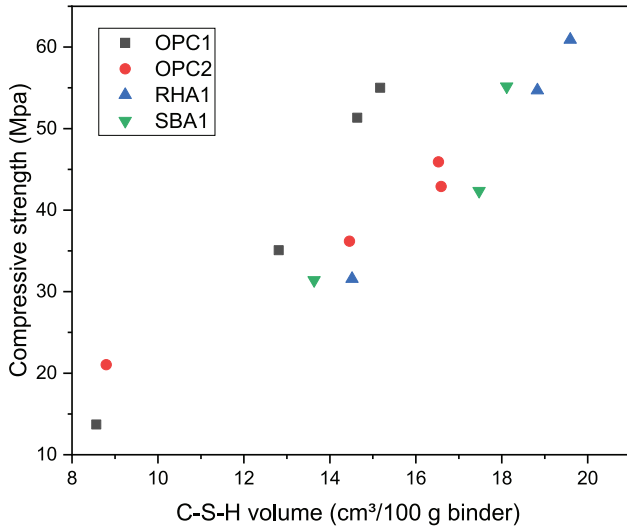


Fig. 5a – CSH gel volume compared to compressive strength

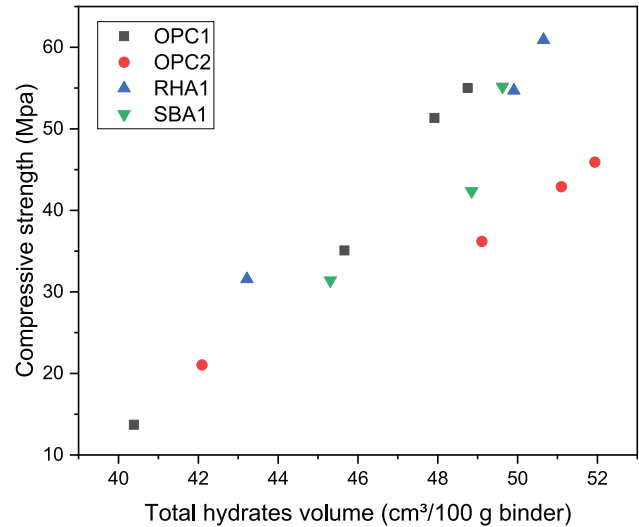


Fig. 5b – Total hydrate volume compared to compressive strength

hydrate volume was not proportionate, indicating that RHA-infused pastes harbor greater pore volume than pure Portland cement pastes. This seemingly paradoxical result may be ascribed to the complex void structure of RHA-blended mixtures, typified by a reduced number of large capillary pores and a greater number of fine pores compared to cement pastes. Consequently, they demonstrated increased compressive strength, even with greater overall porosity.

The recorded Portland cement compressive strength and the blends correspond with the calculated quantity of CSH crystals in Fig. 5a. However, a more robust association emerges when comparing mechanical strength with the overall quantity of residual phases and crystals (Fig. 5b). The cement paste strength is affected by several factors, such as the quantity and nature of formed hydration compounds, the degree of reaction, and the microstructural characteristics of the paste. Although the presence of CSH formations is pivotal for calculating the strength of cement paste, the collective volume of all phases and crystals generated during hydration, including inactive or partially reacted cement particles, CH, and ettringite, also plays a critical role.

## Conclusions

The chemical and mineral characteristics of Portland cement play a significant role in shaping the type and amount of hydrates formed in both OPCs and blends incorporating RHA and SBA. Thermodynamic modeling, aligned with empirical findings on hydrate production, underscored substantial disparities between binary blends and pure

cement, manifesting in increased CSH gel formation, reduced portlandite composition, and the emergence of additional mono-carbonate varying according to the composition of OPC.

While there were minor variations between experimental observations and model outcomes, these disparities may have arisen from sample carbonation during hydration or the incorporation of aluminum in CSH, factors not accounted for in the predictions. Furthermore, the predicted reduced concentration of CSH in composite blends, as per thermodynamic modeling, exhibited a moderately weak correlation with the assessed compressive strength. In contrast, the total crystal volume, encompassing both hydrated components and unreacted materials, demonstrated a stronger association, stressing that the primary factor influencing compressive strength was the total volume of the solid structure, not limited to the CSH portion. Furthermore, this underscores the greater impact of substituting Portland cement with SBA on binary mixes containing RHA.

## References

- Juenger, M. C. G., Snellings, R., Bernal, S. A., Supplementary cementitious materials: New sources, characterization, and performance insights, *Cem. Concr. Res.* **122** (2019) 257.  
doi: <https://doi.org/10.1016/j.cemconres.2019.05.008>
- Cyr, M., Influence of supplementary cementitious materials (SCMs) on concrete durability. In: *Eco-Efficient Concrete*. Elsevier Ltd. (2013) 153.  
doi: [10.1533/9780857098993.2.153](https://doi.org/10.1533/9780857098993.2.153)
- Scrivener, K. L., John, V. M., Gartner, E. M., Eco-efficient cements: Potential economically viable solutions for a low-CO<sub>2</sub> cement-based materials industry, *Cem. Concr. Res.* **114** (2018) 2.  
doi: <https://doi.org/10.1016/j.cemconres.2018.03.015>

4. *Holmes, N., Kelliher, D., Tyrer, M.*, Thermodynamic Cement Hydration Modelling Using HYDCEM. <https://arrow.tudublin.ie/engschcivcon>
5. *Lothenbach, B., Le Saout, G., Gallucci, E., Scrivener, K.*, Influence of limestone on the hydration of Portland cements, *Cem. Concr. Res.* **38** (2008) 848. doi: <https://doi.org/10.1016/j.cemconres.2008.01.002>
6. *Holmes, N., Tyrer, M., Kelliher, D.*, Thermodynamic modelling of harsh environments on the solid phase assemblage of hydrating cements using PHREEQC, *Applied Sciences (Switzerland)* **13** (2023). doi: <https://doi.org/10.3390/app13010135>
7. *Ajeesh Kumar, N. S., Radhika, K. L.*, Thermodynamic modeling of cementitious paste containing sugarcane bagasse ash and rice husk ash, In: Pancharathi, R.K., K. Y. Leung, C., Chandra Kishen, J.M. (Eds.) *Low Carbon Materials and Technologies for a Sustainable and Resilient Infrastructure. CBKR 2023. Lecture Notes in Civil Engineering*, vol 440. Springer, Singapore. doi: [https://doi.org/10.1007/978-981-99-7464-1\\_7](https://doi.org/10.1007/978-981-99-7464-1_7)
8. *Fernández, García Calvo, J. L., Alonso, M. C.*, Ordinary Portland cement composition for the optimization of the synergies of supplementary cementitious materials of ternary binders in hydration processes, *Cem. Concr. Compos.* **89** (2018) 238. doi: <https://doi.org/10.1016/j.cemconcomp.2017.12.016>
9. *Lothenbach, B., Matschei, T., Möschner, G., Glasser, F. P.*, Thermodynamic modelling of the effect of temperature on the hydration and porosity of Portland cement, *Cem. Concr. Res.* **38** (2008) 1. doi: <https://doi.org/10.1016/j.cemconres.2007.08.017>
10. *Lothenbach, B., Winnefeld, F.*, Thermodynamic modelling of the hydration of Portland cement, *Cem. Concr. Res.* **36** (2006) 209. doi: <https://doi.org/10.1016/j.cemconres.2005.03.001>
11. *Parrot, L. J., Killoh, D. C.*, Prediction of cement hydration, *Br. Ceram. Proc.* **35** (1984) 41.
12. *Kulik, D. A., Wagner, T., Dmytrieva, S. V., Kosakowski, G., Hingerl, F. F., Chudnenko, K. V., Berner, U. R.*, GEM-Selector geochemical modeling package: Revised algorithm and GEMS3K numerical kernel for coupled simulation codes, *Comput. Geosci.* **17** (2013) 1. doi: <https://doi.org/10.1007/s10596-012-9310-6>
13. *Lothenbach, B., Kulik, D. A., Matschei, T., Balonis, M., Baquerizo, L., Dilnesa, B., Miron, G. D., Myers, R. J.*, Cemdata18: A chemical thermodynamic database for hydrated Portland cements and alkali-activated materials, *Cem. Concr. Res.* **115** (2019) 472. doi: <https://doi.org/10.1016/j.cemconres.2018.04.018>
14. *Cordeiro, G. C., Kurtis, K. E.*, Effect of mechanical processing on sugar cane bagasse ash pozzolanicity, *Cem. Concr. Res.* **97** (2017) 41. doi: <https://doi.org/10.1016/j.cemconres.2017.03.008>
15. *Bogue, R. H.*, Calculation of the compounds in Portland cement, *Industrial & Engineering Chemistry Analytical Edition* **1** (1929) 192. doi: <https://doi.org/10.1021/ac50068a006>
16. *Taylor, H. F. W.*, Modification of the bogue calculation, *Advances in Cement Research* **2** (1989) 73. doi: <https://doi.org/10.1680/adr.1989.2.6.73>
17. *Abdul, W., Rößler, C., Kletti, H., Mawalala, C., Pisch, A., Bannerman, M. N., Hanein, T.*, On the variability of industrial Portland cement clinker: Microstructural characterisation and the fate of chemical elements, *Cem. Concr. Res.* **189** (2025). doi: <https://doi.org/10.1016/j.cemconres.2024.107773>
18. *Shim, S. H., Lee, T. H., Yang, S. J., Noor, N. B. M., Kim, J. H. J.*, Calculation of cement composition using a new model compared to the bogue model, *Materials* **14** (2021) 1. doi: <https://doi.org/10.3390/ma14164663>
19. *Schöler, A., Lothenbach, B., Winnefeld, F., Haha, M. B., Zajac, M., Ludwig, H. M.*, Early hydration of SCM-blended Portland cements: A pore solution and isothermal calorimetry study, *Cem. Concr. Res.* **93** (2017) 71. doi: <https://doi.org/10.1016/j.cemconres.2016.11.013>
20. *Snellings, R., Chwast, J., Cizer, Ö., De Belie, N., Dhandapani, Y., Durdzinski, P., Elsen, J., Haufe, J., Hooton, D., Patapy, C., Santhanam, M., Scrivener, K., Snoeck, D., Steger, L., Tongbo, S., Vollpracht, A., Winnefeld, F., Lothenbach, B.*, RILEM TC-238 SCM recommendation on hydration stoppage by solvent exchange for the study of hydrate assemblages, *Materials and Structures/Materiaux et Constructions* **51** (2018) 6. doi: <https://doi.org/10.1617/s11527-018-1298-5>
21. *Scrivener, K., Snellings, R., Lothenbach, B.*, (Eds.) *A Practical Guide to Microstructural Analysis of Cementitious Materials*. 1st Edition. CRC Press, 2018, pp 420–452. doi: <https://doi.org/10.1201/b19074>
22. *Soin, A. V., Catalan, L. J. J., Kinrade, S. D.*, A combined QXRD/TG method to quantify the phase composition of hydrated Portland cements, *Cem. Concr. Res.* **48** (2013) 17. doi: <https://doi.org/10.1016/j.cemconres.2013.02.007>
23. *Kulik, D. A.*, Improving the structural consistency of C-S-H solid solution thermodynamic models, *Cem. Concr. Res.* **41** (2011) 477. doi: <https://doi.org/10.1016/j.cemconres.2011.01.012>
24. *Fernandez, A., Alonso, M. C., García-Calvo, J. L., Lothenbach, B.*, Influence of the synergy between mineral additions and Portland cement in the physical-mechanical properties of ternary binders, *Materiales de Construcción* **66** (2016) 324. doi: <https://doi.org/10.3989/mc.2016.10815>
25. *Lothenbach, B.*, Thermodynamic equilibrium calculations in cementitious systems, *Materials and Structures/Materiaux et Constructions* **43** (2010) 1413. doi: <https://doi.org/10.1617/s11527-010-9592-x>